

# Cold quantum gases: coherent quantum phenomena from Bose-Einstein condensation to BCS pairing of fermions

Gordon Baym

*Department of Physics, University of Illinois at Urbana-Champaign, 1110 West Green Street, Urbana, IL 61801*

(Dated: January 11, 2019)

Studies of trapped quantum gases of bosons and of fermions have opened up a new range of many-body problems, having a strong overlap with nuclear and neutron star physics. Topics discussed here include: the Bose yrast problem – how many-particle Bose systems carry extreme amounts of angular momentum; the infrared divergent structure of the transition to Bose condensation in a weakly interacting system; and the physics of extremely strongly interacting Bose and Fermi systems, in the scale-free regime where the two body s-wave scattering lengths are large compared with the interparticle spacing. Such a regime is realized experimentally through use of atomic Feshbach resonances. Finally we discuss creation of BCS-paired states in trapped Fermi gases.

## I. INTRODUCTION

The past decade has seen remarkable developments in the study of the physics of ultracold trapped quantum atom gases. Below a certain critical temperature, Bose systems become Bose-Einstein condensed superfluids, with a macroscopic fraction of the particles occupying the lowest single particle mode of the system. In 1995 the first Bose-Einstein condensed gases of bosonic alkali atoms were produced [1, 2, 3]. In the past several years considerable attention has focussed on cooling fermionic alkali atoms to the point where they become degenerate [4, 5] and indeed undergo BCS pairing [6, 7, 8, 9]. These laboratory phenomena in ultracold trapped quantum gases have a strong overlap with nuclear and neutron star physics. In this talk, I would like give an overview of the field, and indicate why this area has become so challenging to nuclear physicists.

The ideas of Bose-Einstein condensation (BEC) have played an important role over the years in understanding the properties of the vacuum and of matter under extreme conditions. Condensates of  $\pi$  mesons [10] and of K mesons [11] have been studied as possible states of neutron star matter. Bosonic condensates, e.g., with non-vanishing expectation values of quark operators,  $\langle \bar{u}u \rangle$ ,  $\langle \bar{d}d \rangle$ ,  $\langle \bar{s}s \rangle$ , are fundamental features of the vacuum and the structure of elementary particles such as the nucleon, and underly the spontaneous breaking of the chiral symmetry of the strong interactions [12]. One of the important aims of ultrarelativistic heavy ion collisions at RHIC (and soon at LHC) is to produce chirally restored matter in the form of quark-gluon plasmas; there one is asking the opposite of the question asked in condensed matter physics, namely, what are the properties of Bose-Einstein *de*-condensed matter [13]. Bose condensation of Cooper pairs is familiar in nuclear physics, where BCS pairing explains reduced moments of inertia of heavier nuclei. Both the neutron and proton components of neutron star matter, more generally, undergo BCS pairing to become superfluid. Such superfluidity most likely underlies the observed glitches, or sudden rotational speedups, observed in some 30 pulsars to date [14, 15].

Experiments in atomic systems are done primarily on vapors of alkali metal atoms. The alkalis have one electron outside a close shell and an odd number of protons; thus the statistics a given isotope obeys is governed by whether the nucleus has an even number of neutrons, in which case the atom is a boson, or odd, in which case it is a fermion. Since odd-odd nuclei tend to be unstable, most alkali atoms are bosons. The principal actors in the study of atomic Bose-Einstein condensates are  $^{87}\text{Rb}$  (half-life,  $T_{1/2} = 4.75 \times 10^{10}\text{y}$ ) and  $^{23}\text{Na}$ ; condensates of  $^7\text{Li}$  have also been studied, but the effective low energy interactions between  $^7\text{Li}$  are attractive, which limited the number of atoms that could be assembled in a vapor. Two fermionic alkalis are long enough lived to be readily used in trapping experiments,  $^6\text{Li}$ , which is stable, and  $^{40}\text{K}$ , with  $T_{1/2} = 1.3 \times 10^9\text{y}$ . Typical clouds contain  $\sim 10^6$  atoms, with density  $\sim 10^{14}/\text{cm}^3$ , cooled via a combination of laser and then evaporative cooling, to temperatures  $\sim 10^{-8}\text{K}$ , the coldest systems in the universe!

Because the temperatures are so very low, with typical atomic velocities of order mm/s, the two particle interatomic interactions are low energy s-wave, described by a pseudopotential,

$$v_{int}(\vec{r}_1 - \vec{r}_2) = g\delta(\vec{r}_1 - \vec{r}_2), \quad (1)$$

where  $g = 4\pi\hbar^2 a_s/m$ , with  $a_s$  the s-wave scattering length. The first generation of Bose-Einstein condensation experiments focussed on phenomena described accurately within mean-field theory, via the Gross-Pitaevskii equation [16],

$$i\hbar \frac{\partial}{\partial t} \Psi(\vec{r}, t) = -\frac{\hbar^2}{2m} \nabla^2 \Psi(\vec{r}, t) + V(\vec{r})\Psi(\vec{r}, t) + g|\Psi(\vec{r}, t)|^2 \Psi(\vec{r}, t), \quad (2)$$

for the condensate wave function,  $\Psi(\vec{r}, t) = \langle \psi(\vec{r}, t) \rangle$ . Here  $\psi$  is the single particle annihilation operator, and  $V$  is the external trapping potential. Such studies included the shape of the condensate (primarily described by Thomas-Fermi theory) [17], the elementary modes – breathing, quadrupole oscillations [18], shorter wavelength sound propagation, and scissor modes, in which the atomic cloud undergoes angular oscillations with respect an asymmetric trap, the analogue of angular counter-oscillations of the neutron and proton clouds in nuclei.

Studies of two-body correlations,  $\langle \psi^\dagger \psi^\dagger \psi \psi \rangle$ , through measurements of the interaction energy, and three-body correlations  $\langle \psi^\dagger \psi^\dagger \psi^\dagger \psi \psi \psi \rangle$ , through measurements of rates at which three atoms “recombine” into a molecule and fast atom, provided direct evidence that the systems were Bose-condensed and not simply condensed in space, e.g., in a normal weakly interacting gas,

$$\langle \psi^\dagger \psi^\dagger \psi \psi \rangle = 2 \langle \psi^\dagger \psi \rangle^2, \quad (3)$$

and

$$\langle \psi^\dagger \psi^\dagger \psi^\dagger \psi \psi \psi \rangle = 6 \langle \psi^\dagger \psi \rangle^3, \quad (4)$$

while in a condensate the factors of two and six are, as predicted and observed, absent. Noteworthy is the measurement of Ref. [19] of the single particle correlation function  $\langle \psi^\dagger(\vec{r}) \psi(\vec{r}') \rangle$  in trapped  $^{87}\text{Rb}$ , which below the transition temperature extends to a finite value at large  $|\vec{r} - \vec{r}'|$ , as predicted for a Bose-condensed superfluid, but never actually observed in superfluid  $^4\text{He}$ .

The first experiment to demonstrate directly the quantum coherence of Bose condensates is that at MIT of Andrews et al. [20]. This experiment cooled two independent atomic systems to below the transition temperature, and then released them so that they expanded into each other, exhibiting quantum interference, analogous to the interference of two classical electromagnetic waves from independent sources.

In the past several years, the field has undergone dramatic expansion, as experiment has gone into new regimes, including strong coupling and trapped fermions. The enticement of trapping fermions is the possibility of producing BCS paired superfluids of atoms. Trapped bosons and fermions behave similarly at high temperatures. At low temperatures, condensed bosons fall to the center of the trap, limited only by the uncertainty principle, while trapped fermionic clouds below the Fermi degeneracy temperature,  $T_f$ , are supported at larger radii by Fermi degeneracy pressure. Current temperatures achieved in Fermi systems are as low as a few percent of  $T_f$  [6], in systems of some  $10^6$  atoms. Through rapid rotation, discussed below, one is able to produce lattices of vortices, and study the Bose yrast problem, how many-particle Bose systems carry extreme amounts of angular momentum. By means of optical lattices – formed by counter-propagating lasers producing standing electromagnetic waves – one can control to an unprecedented degree the environment in which the atoms sit. For example, one can produce lattices in one, two and three dimensions. By increasing the lattice depth one can change a system from a superfluid to a Mott insulator [21]. By means of Feshbach resonances in two particle scattering, discussed below, one is able to control the strength and sign of the interaction between particles, and thus dial the system into the strong coupling regime at will. The latter technique has enabled one to produce fermion systems in the BCS paired regime and then follow their evolution, as the interaction is changed from attractive to repulsive, into the regime where the atoms form a Bose condensate of molecules. Among other areas of present interest are production of coherent mixtures of atoms and molecules, spinor gases, fragmented condensates, and mixtures of bosons and fermions.

## II. RAPIDLY ROTATING BOSE CONDENSATES

Understanding how Bose-Einstein condensates carry extreme amounts of angular momentum explores regimes of many-body physics not encountered in other systems [22]. As one rotates a Bose condensate rapidly, it forms a triangular array of singly quantized vortex lines [23, 24, 25, 26, 27]. The angular momentum of the system is  $\sim N_v N \hbar$ , where  $N$  is the total number of particles in the system, and  $N_v$  is the number of vortices present (as large as  $\sim 300$  experimentally). The superfluid velocity,  $\vec{v}$ , obeys the quantization condition,

$$\oint \vec{v} \cdot d\vec{\ell} = (h/m) N_v(\mathcal{C}), \quad (5)$$

where the line integral is along a closed contour surrounding  $N_v(\mathcal{C})$  singly quantized vortices, and  $m$  is the particle mass. The velocity in the neighborhood of a single line is in the azimuthal direction and has magnitude  $\hbar/m\rho$ , where  $\rho$  is the distance from the line. A system containing many vortex lines appears to rotate uniformly with an average angular velocity  $\Omega$ , which is simply related to the (two-dimensional) density of vortex lines,  $n_v$ , by the quantization condition:  $\Omega = \pi \hbar n_v / m$ . As the system rotates more and more rapidly, the lines become closer and closer. What eventually happens to the system as the angular momentum grows to the range of  $10^2 N \hbar$  to  $N^2 \hbar$ ?

Type II superconductors in the presence of a magnetic field above a critical value,  $H_{c1}$ , contain an array of vortex lines with quantized flux. With increasing field the line density grows until the cores begin to overlap, at a critical field,  $H_{c2}$ , at which point the system turns normal. However, a low temperature rotating bosonic system does not have a normal phase to which it can return. Unlike in a weakly interacting superconductor, where condensation occurs as a small dynamical decoration on top of a normal state, Bose condensation occurs kinematically. A Bose system must respond differently than a Type II superconductor. In a weakly interacting atomic condensate, the radius of a single vortex core is of order  $\xi_0 = 1/\sqrt{8\pi n a_s}$ , where  $n$  is the particle density. Typically,  $\xi_0 \sim 0.2 \mu\text{m}$ , so that cores would begin to touch at  $\Omega_{c1} \sim 8\pi^2 n a_s \hbar/m \sim 10^3 - 10^5$  rad/sec, an experimentally accessible rate.

The ground state of the system rotating at angular frequency  $\Omega$  about the  $z$  axis is determined by minimizing the energy in the rotating frame,  $E' = E - \Omega L_z$ , where  $L_z$  is the component of the angular momentum of the system along the rotation axis:

$$E' = \int d^3r \left[ \frac{\hbar^2}{2m} \left| (-i\nabla - m\vec{\Omega} \times \vec{r}) \Psi \right|^2 + \left( V(\vec{r}) - \frac{1}{2}m\Omega^2 r_\perp^2 \right) |\Psi|^2 + \frac{1}{2}g|\Psi|^4 \right], \quad (6)$$

and  $\vec{r}_\perp = (x, y)$ .

The fate of a rapidly rotating Bose system depends on how the system is confined. In typical condensate experiments the system, rotating about the  $z$  axis, is confined in a harmonic trap of the form,

$$V(r_\perp, z) = \frac{1}{2}m(\omega_\perp^2 r_\perp^2 + \omega_z z^2). \quad (7)$$

In this case the centrifugal potential,  $-\frac{1}{2}m\Omega^2 r_\perp^2$ , tends to cancel the transverse trapping potential, and the system cannot rotate faster than  $\omega_\perp$  without becoming untrapped. As  $\Omega \rightarrow \omega_\perp$ , the system flattens out, becomes almost two dimensional, and eventually enters quantum Hall-like states. The interesting physics begins in the regime  $\Omega/\omega_\perp \gtrsim 0.9$ ; current experiments [26, 27] have reached  $\Omega/\omega_\perp \approx 0.995$ . The limit  $\Omega < \omega_\perp$  is analogous to that in relativistic physics, where particles velocities are bounded by the speed of light. It is thus useful to measure such rapid rotational rates in terms of a corresponding *rotational rapidity* [28], defined by

$$\tanh y = \Omega/\omega_\perp, \quad y = \frac{1}{2} \ln \left| \frac{\omega_\perp - \Omega}{\omega_\perp + \Omega} \right|, \quad (8)$$

which conveniently spreads out the region where  $\Omega \lesssim \omega_\perp$ .

The physics in the presence of an anharmonic transverse trapping potential that grows faster than quadratic, e.g.,

$$V_\perp(r_\perp) = \frac{1}{2}m\omega_\perp^2 r_\perp^2 (1 + \lambda r_\perp^2), \quad (9)$$

is quite different, since, the system, being contained by the anharmonic part of the potential, can rotate faster than  $\omega_\perp$ .

### A. Shrinking vortex cores

In fact there is never a phase transition associated with the vortex cores overlapping in a rotating Bose condensate. Rather, as was shown in Ref. [29] and later [28] in a variation treatment of the core radius,  $\xi$ , the vortex cores begin to shrink as the intervortex spacing becomes comparable to the mean field coherence length,  $\xi_0$ , and eventually the core radius scales down with the intervortex spacing. Figure 1a shows the resultant mean square area of the vortex core, in a harmonic trap, measured in units of the area per vortex line, for the qualitatively accurate model in which the condensate wave function has the form  $\Psi(\rho) \sim \rho$ , for  $\rho < \xi$ , and constant for  $\xi < \rho < \ell$ , where  $\ell$  is the radius of the (cylindrical) Wigner-Seitz cell around a given vortex:  $\ell^2 = 1/m\Omega$ . In this model, the mean square core area divided by the area per vortex,  $\mathcal{A}$ , is  $\xi^2/3\ell^2$ . The horizontal axis in Fig. 1a is the rotational rapidity,  $y$ . The linear rise at small  $\Omega$  occurs because the core size remains constant, while  $\ell^2$  decreases linearly with  $1/\Omega$ . The flattening of  $\mathcal{A}$  with increasing  $\Omega$  is a consequence of the vortex radius scaling with the intervortex spacing. The upper line shows the exact lowest Landau level limit (described below) as  $\Omega \rightarrow \omega_\perp$ . Recent JILA measurements [26, 27] of  $\mathcal{A}$  (as a function of  $2\hbar\Omega/gn$ ), Fig. 1b, nicely show the expected initial linear rise, followed by the predicted scaling of the core radius with intervortex spacing.

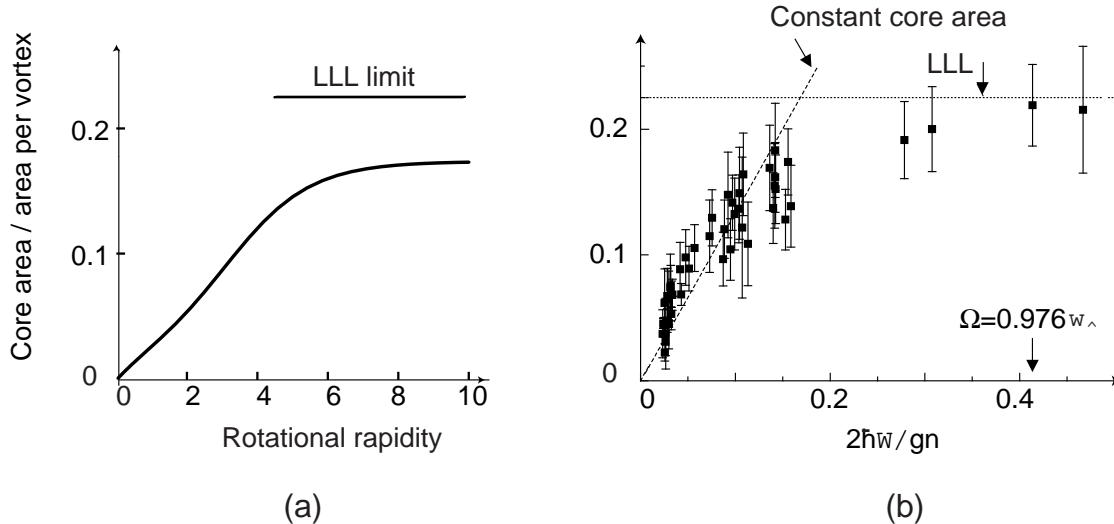


FIG. 1: (a) Mean vortex core area as a fraction of the area per vortex vs. the rotational rapidity (see text). (b) Measured vortex core area as a fraction of the area per vortex vs.  $2\hbar\omega/gn$  (adapted, with permission, from Ref. [26]).

### B. Lowest Landau level regime

As the rotation rate in a harmonic trap approaches  $\omega_{\perp}$ , the centrifugal potential basically cancels the transverse trapping potential; the cloud flattens out, and becomes an effectively two dimensional system. Because the density  $n$  of the system drops, the interaction terms  $\sim gn$ , become small compared with  $\hbar\Omega$ . Then, as one sees from Eq. (6) with (7), the dynamics is that of a particle feeling the Coriolis force alone, a system formally analogous to a particle in a magnetic field. Ho [30] predicted that in this limit particles should condense into the lowest Landau level (LLL) in the Coriolis force, similar to charged particles in the quantum Hall regime. When  $2gn \ll \Omega$ , the states in the next higher Landau level are separated by a gap  $\simeq 2\omega_{\perp}$ . This insight has led to extensive experimental studies [24, 26].

The single particle wave functions in the lowest Landau level have the form,

$$\phi_{\mu}(\vec{r}_{\perp}) \sim \zeta^{\mu} e^{-r_{\perp}^2/2d_{\perp}^2}, \quad (10)$$

where  $\zeta = x + iy$ ,  $\mu = 0, 1, 2, \dots$ , and the transverse oscillator length,  $d_{\perp}$ , is given by  $\sqrt{\hbar/m\omega_{\perp}}$ . The LLL condensate wave function is a linear superposition of such states:

$$\Psi_{\text{LLL}}(\vec{r}_{\perp}) \sim \sum_{\mu} c_{\mu} \zeta^{\mu} e^{-r^2/2d_{\perp}^2} \sim \prod_{i=1}^N (\zeta - \zeta_i) e^{-r^2/2d_{\perp}^2}, \quad (11)$$

where in the latter form the polynomial  $\sum_{\mu} c_{\mu} \zeta^{\mu}$  is written as a product over its zeroes,  $\zeta_i$ , which are simply the positions of the vortices in the condensate. The state (11) in the regime  $gn \ll \hbar\Omega$  is a direct continuation of the state in the slowly rotating regime,  $\hbar\Omega \ll gn$ .

As long as the total number of vortices is much larger than unity, the energy of the cloud in the LLL limit is given by [31]

$$E' = \Omega N + \int d^3r \left\{ (\omega_{\perp} - \Omega) \frac{r_{\perp}^2}{d_{\perp}^2} n(\vec{r}) + \frac{bg}{2} n(\vec{r})^2 \right\}, \quad (12)$$

plus terms involving the trapping potential in the  $z$  direction. Here  $n(\vec{r})$  is the smoothed density profile,  $= \langle |\Psi_{\text{LLL}}|^2 \rangle$ ; the brackets denote the long wavelength smoothing. The energy (12) is minimized when the cloud assumes a density profile of the Thomas-Fermi form [17],

$$n(r_{\perp}) \sim (1 - r_{\perp}^2/R^2), \quad (13)$$

an inverted parabola, where  $R$  is the transverse radius of the cloud. For  $Na/d_z \gg 1$ , where  $d_z$  is the axial oscillator length, the structure in the radial direction will be Thomas-Fermi at large  $\Omega$ , even if it is Gaussian at small  $\Omega$  [28]. In experiment [26, 27], the density profile indeed remains an inverted parabola as  $\Omega \rightarrow \omega_{\perp}$ .

Since the energy (12) depends only on the smoothed density, the vortices must adjust their locations in order that the smoothed density be an inverted parabola. From the arguments in Ref. [30], we find the relation between the smoothed density and the mean vortex density,  $n_v(r_\perp)$ ,

$$\frac{1}{4}\nabla^2 \ln n(r_\perp) = -\frac{1}{d_\perp^2} + \pi n(r_\perp). \quad (14)$$

For a Gaussian density profile, the vortex density is constant. However, for a Thomas-Fermi profile (13),

$$n_v(r_\perp) = \frac{1}{\pi d_\perp^2} - \frac{1}{\pi R^2} \frac{1}{(1 - r_\perp^2/R^2)^2}. \quad (15)$$

Since the second term is of order  $1/N_v$  compared with the first, the density of the vortex lattice is basically uniform (and the vortex array forms an almost perfect triangular lattice). Turning the argument around, very small distortions of the vortex lattice from triangular can result in large changes in the density distribution. Recent measurements of the (percent scale) distortions of the vortex lattice at relatively low rotation rates [27] are in good agreement with theory.

### C. Beyond the LLL regime

At sufficiently high rotation, the vortex lattice should melt and become a vortex liquid. The regime just beyond melting has yet to be described in detail. At still higher rotation speeds in harmonic traps, as seen in numerical simulations with a limited number of particles, the system begins to enter a sequence of highly correlated incompressible fractional quantum Hall-like states [32, 33, 34, 35]. For example, at angular momentum  $L_z = N(N-1)$ , where  $N_v$  (measured in terms of the total circulation,  $N_v = (m/h) \oint \vec{v} \cdot d\vec{\ell}$ ) equals  $2N$ , the exact ground state is an  $N$ -particle fully symmetric Laughlin wave function (in two dimensions),

$$\Psi(r_1, r_2, \dots, r_N) \sim \prod_{i \neq j} (\zeta_i - \zeta_j)^2 e^{-\sum_k r_k^2 / 2d_\perp^2}, \quad (16)$$

where  $\zeta_j = x_j + iy_j$ . Since the wave function vanishes whenever two particles overlap, the interaction energy,  $\frac{1}{2}g\sum_{i \neq j} \delta(\vec{r}_i - \vec{r}_j)$ , vanishes in this state. Theoretically elucidating the states in general when the angular momentum per particle is of order the total particle number, as well as studying this regime experimentally, remain important challenges.

### D. Anharmonic traps

The physics of a condensate confined in an anharmonic trap, e.g., (9), is quite different from that in a harmonic trap, since it becomes possible to rotate the system arbitrarily fast. As the system rotates sufficiently rapidly, the centrifugal force pushes the particles towards the edge of the trap, and a hole opens up in the center. Singly quantized vortex arrays with a hole have been seen in numerical simulations [36] and discussed theoretically in Refs. [29] and [37]. In addition, at very high rotation, systems tend to form a single multiply quantized vortex at the center, with order parameter  $\psi \sim e^{i\nu\phi}$ , where the integer quantization index  $\nu$  is  $\gg 1$ . Such giant vortices have been seen in numerical simulations [36, 38], and are discussed theoretically in Refs. [29] and [37]. The schematic phase diagram, as a function of interparticle interaction strength vs. rotation rate is shown in Fig. 2. Full details can be found in Refs. [37]. Initial studies of rapidly rotating condensates in harmonic lattices at the ENS are reported in Ref. [39].

## III. DEPENDENCE OF THE TRANSITION TEMPERATURE ON THE SCATTERING LENGTH

The problem of determining the effects of a weak interaction, described by an s-wave scattering length,  $a_s > 0$ , on the Bose-Einstein condensation transition temperature in a uniform system has had a long and tortured history (reviewed in [40]) [41]. The problem is of great interest to nuclear physicists since it is a system plagued by infrared divergences, albeit not as severe as those encountered in quark-gluon plasmas. The result for the transition temperature, as finally resolved in [40], is that for small  $a_s n^{1/3}$  the shift in the transition temperature is linear in  $a_s$  and positive:

$$\frac{\Delta T_c}{T_c^0} = c a_s n^{1/3}, \quad (17)$$

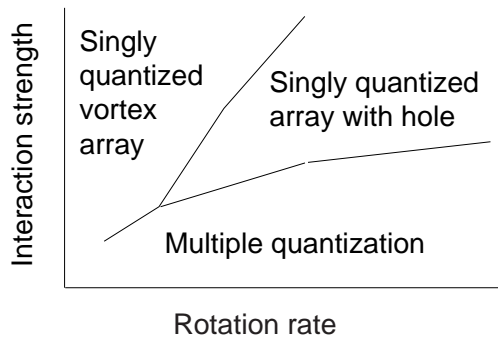


FIG. 2: Schematic phase diagram of the ground state of a rapidly rotating Bose condensed gas at zero temperature in the  $\Omega$ - $Na_s/Z$  plane, where  $Z$  is the height in along the rotation axis, showing the regions of multiply quantized vortices, of singly quantized vortices forming an array which at large number becomes a triangular lattice, and of an array of singly quantized vortices with a hole in the center.

where  $T_c^0$  is the free gas transition temperature, given by  $\zeta(3/2)\lambda^{-3}$ , with thermal wavelength  $\lambda = (2\pi\hbar^2/m\kappa_B T)^{-1/2}$ , and  $T_c = T_c^0 + \Delta T_c$  is the transition temperature in the presence of interactions. The positive constant  $c$  is of order 1-2, but cannot be calculated in closed form. Because the low energy s-wave interparticle interaction,  $\sim 4\pi\hbar^2 a_s/m$ , is first order in  $a_s$ , it would appear at first glance that the result (17) should be straightforward to derive. However, the first order, or mean field shift, in the particle energies has no effect on the transition temperature, since it is independent of momentum and thus compensated by a shift in the chemical potential. In second and higher order in the dimensionless expansion parameter  $a_s/\lambda$ , each and every term in the perturbation expansion involves integrals that diverge in the infrared, implying that to find a finite answer one has to sum an infinite set of terms. The problem is a true critical phenomenon, completely outside the range of Gross-Pitaevskii mean field.

Successful approaches to the problem have been three-fold. The first is via numerical simulation of finite systems, including path integral Monte-Carlo calculations [42, 43], and more recent calculations of  $\phi^4$  field theory on the lattice, extrapolated to the continuum limit [44, 45]. The second has been through analysis of the scaling structure of the perturbation expansion in finite temperature field theory [40]. A third approach has been by means of the renormalization group, carried out for a field theory with  $N$  components (compared to the two components corresponding to the real and imaginary parts of the order parameter  $\Psi$ ) in [46]; in the limit where the number of components goes to  $\infty$  the exact result for the shift in the transition temperature is  $c = 8\pi/3\zeta(3/2)^{4/3} = 2.33$ . In a trapped Bose gas, the finite level spacing regulates the infrared divergences;  $T_c$  decreases because the interparticle interactions lower the density. With interaction effects, as calculated by Arnold and Tomášik [47], the relative shift is  $\sim 3.4a_s/\lambda$ , where  $\lambda$  measures the interparticle spacing in the center of the trap.

Interestingly, the various calculations of  $c$  in a homogeneous gas differ noticeably, ranging from  $0.34 \pm 0.06$  [42] to  $\simeq 1.3$  [44, 45]), to  $2.33 \pm 0.25$  [43]. The discrepancy has a physical origin, namely that the expansion of  $\Delta T_c/T_c^0$  in powers of  $a_s/\lambda$  has a highly non-analytic structure. In fact, the series cannot be analytic, since an infinite homogeneous system of bosons with negative  $a_s$  is unstable against collapse. Were the series analytic about zero scattering length, it would have to hold for sufficiently small  $|a_s|$ , whether  $a_s$  is positive or negative. Rather, the series is asymptotic for positive small  $a_s$ . As shown in [48], to next leading order the series has the form

$$\frac{\Delta T_c}{T_c^0} = c(a_s n^{1/3}) + d(a_s n^{1/3})^2 \ln(a_s n^{1/3}) + \mathcal{O}\left(\left((a_s n^{1/3})^2\right)\right), \quad (18)$$

with  $d$  positive. The logarithmic term introduces rapid variation of  $\Delta T_c/T_c^0$  with  $a_s$ . In the limit of large  $N$ ,

$$\frac{\Delta T_c}{T_c} = \frac{8\pi}{3\zeta(3/2)} \frac{a_s}{\lambda} \left\{ 1 + 16N \frac{a_s}{\lambda^2 \Lambda} \ln \frac{Na_s}{\lambda^2 \Lambda} + \mathcal{O}\left(\frac{Na_s}{\lambda^2 \Lambda}\right) \right\}, \quad (19)$$

where  $\Lambda \sim 1/\lambda$  is the effective ultraviolet cutoff in a calculation within classical field theory near  $T_c$ . The coefficient of the logarithmic term has been calculated exactly by Arnold et al. [49], who find  $d \simeq 19.7518$ ; the logarithmic term in Eq. (19) for  $N = 2$  and  $\Lambda \sim \sqrt{2\pi}/\lambda$  is in reasonable agreement with this exact result. The logarithmic term reduces the shift by about a factor of two for  $a_s n^{1/3} \sim 10^{-2}$  and by a factor of order six for  $a_s n^{1/3} \sim 10^{-2}$ , thereby substantially improving the agreement with the calculations of Ref. [42], for which the lowest data point was at  $a_s n^{1/3} \sim 10^{-2}$ . Quite generally, the logarithmic corrections play an important role in comparison of the various numerical calculations.

#### IV. FESHBACH RESONANCES AND UNIVERSALITY

One enormous advantage enjoyed by experimentalists working with trapped atomic systems is the ability to vary the parameters of the system over ranges inconceivable in other systems. One can readily control the type of atoms, their number and density, and the shape of the trap. Optical lattices permit one to study systems in varying dimensions and confinement. Perhaps the most spectacular freedom of these systems is the ability to control the strength and sign of the interactions between the particles, via Feshbach resonances.

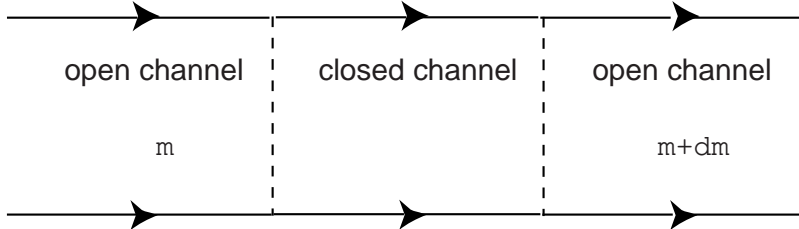


FIG. 3: Two atoms in the initial (open) channel, with total magnetic moment  $\mu$ , scattering through an intermediate state (closed channel) with total magnetic moment  $\mu + \delta\mu$ . When the energies of the intermediate and initial states are tuned via a magnetic field, the scattering has a Feshbach resonance.

In the scattering of two atoms, total angular momentum is conserved. However, the atoms, through the hyperfine interaction, can scatter into intermediate states (Fig. 3) in which one or both atoms are in different hyperfine states. Since the magnetic moment of the atomic states is determined by the valence electron configuration, the net magnetic moment,  $\mu + \delta\mu$ , in the intermediate states can be different from that of the initial state,  $\mu$ . Thus in the presence of a magnetic field,  $B$ , the relative energies of the initial (0) and intermediate (i) states will be shifted by  $\delta\mu B$ . If the intermediate and initial levels cross at a magnetic field,  $B_{res}$ , the two particle scattering amplitude will have a resonance, known as a Feshbach resonance, there. The process in Fig. 3 gives a contribution to the scattering amplitude

$$\delta a_s \sim \frac{|M|^2}{E_0(B) - E_i(B)}, \quad (20)$$

so that  $a_s$  near resonance has the form,

$$a_s(B) = a_b \left( 1 - \frac{\Delta}{B - B_{res}} \right), \quad (21)$$

as shown schematically in Fig. 4, where the background scattering length  $a_b$  is the value of the scattering length away from resonance.

Note that not only does the scattering amplitude diverge at the resonance, it changes sign across the resonance. Thus for the case illustrated in Fig. 4 (for  $\Delta > 0$ , as occurs in both stable fermion alkalis,  ${}^6\text{Li}$  and  ${}^{40}\text{K}$ ) the effective interaction between the atoms changes from repulsive for  $B < B_{res}$  to attractive for  $B > B_{res}$ . To understand the basic physics a useful first picture is to think in terms of the particles interacting via an *attractive* short ranged potential with an s-wave bound state near zero energy. If the bound state is just below zero, then the s-wave scattering length is positive, so that particles at low energy feel a residual repulsion. This situation corresponds to the region in Fig. 4 to the left of the resonance. Decreasing the depth of the potential is equivalent to moving to the right in this figure. As the potential becomes less deep and the bound state approaches zero energy, the scattering length grows, and finally as the bound state moves into the continuum, the scattering length becomes negative, and particles in the continuum attract.

Early experiments employed the Feshbach resonance in bosonic  ${}^{85}\text{Rb}$ , at  $B=155\text{G}$ , to study, e.g., how a cloud initially with a positive scattering length undergoes collapse as the interaction is suddenly made attractive [50]. Currently, Feshbach resonances are being employed to bring Fermi systems into the strongly interacting regime, where one can induce BCS pairing, as well as study the crossover from a Bose condensate of two-fermion molecules to BCS superfluidity.

##### A. Physics at resonance

Away from a Feshbach resonance, the interparticle spacing is generally large compared with the scattering length, i.e.,  $na_s^3 \ll 1$ , where  $n$  is the density, so that the systems can be treated as weakly interacting. Furthermore, the range

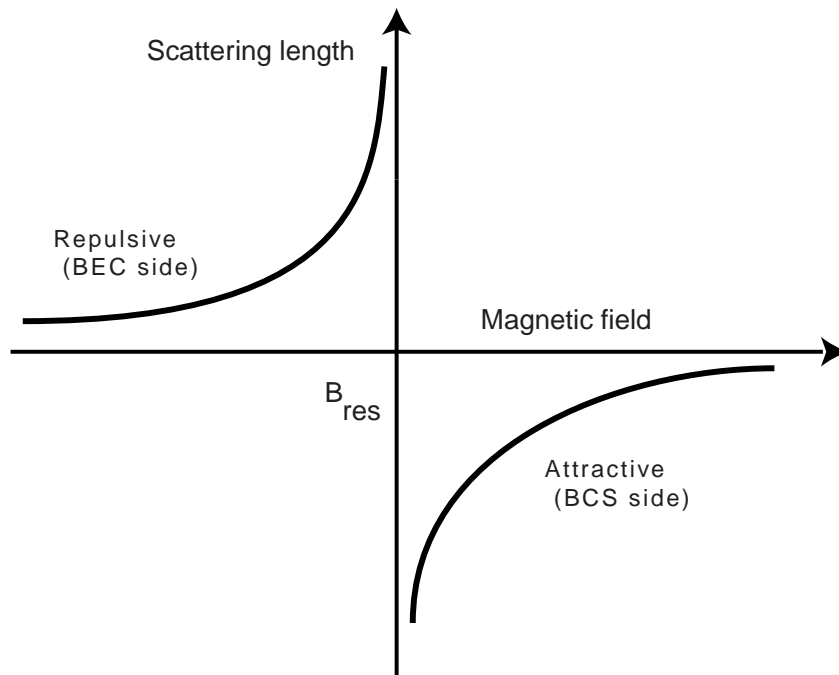


FIG. 4: Scattering length vs. magnetic field in neighborhood of a Feshbach resonance at magnetic field  $B_{res}$ .

of the actual interatomic potentials is small compared with either  $a_s$  or  $n^{-1/3}$ , so that one has a clean separation of length scales. In the neighborhood of a Feshbach resonance, however, the scattering length becomes large compared with the interparticle spacing,  $a_s \gg n^{-1/3}$ , and the system enters a strongly interacting *unitarity* regime. Here the scattering length is an irrelevant parameter, as is the microscopic scale of the interatomic potential. The two-particle s-wave cross section is unitarity limited by  $8\pi/k^2$ , where  $k$  is the relative momentum of the colliding pair. Thus the only relevant length scale in the problem is the interparticle spacing, and the structure of the system should exhibit universality.

In particular, in a system of bosons or fermions, the ground state energy per particle must have the form,  $E/N \sim n^{2/3}/m$ ; one can write,

$$E/N = \frac{3}{5}E_f^0(1 + \beta), \quad (22)$$

where in a Fermi gas the free particle Fermi energy,  $E_f^0$  equals  $k_f^2/2m$ , with  $k_f$  the Fermi momentum, and  $\beta$  is a universal parameter (dependent only on statistics) and non-trivial to calculate. Via a fixed node Monte Carlo method, Carlson et al. [51] derive  $\beta = -0.56$ , while using a lowest order constrained variational calculation, Heiselberg [52] finds  $\beta = -0.33$ . These results, and notably the sign of  $\beta$ , are in reasonable agreement with experimental determinations of the energy via studying the expansion of a cloud released from the trap, e.g., [53, 54].

The expansion of a cloud in the resonant regime exhibits elliptic flow [5], quite similar to that observed in ultra-relativistic heavy ion collisions. Indeed strongly coupled quark-gluon plasmas and strongly coupled atomic fermionic clouds share the feature that both appear to be very nearly perfect fluids [55].

## V. FERMION PAIRING

S-wave pairing in a fermion system, e.g., electrons, or nucleons, normally takes place between particles of opposite spin. However, magnetic traps permit one to trap only the low-field seeking states. Furthermore, the temperatures one can reach are generally too large a fraction of the Fermi temperature for BCS pairing to take place without enhancing the interaction strength. Thus the strategy to achieve pairing in a magnetic trap is to populate equally two hyperfine atomic states, and by means of a Feshbach resonance, strengthen the interaction between them [56]. (Note that owing to the Pauli principle, interactions within a given hyperfine level are very small, since the interactions are very short ranged.)

In the regime to the right of the resonance in Fig 4, where the interactions between particles in the continuum are attractive, one expects fermions in the two hyperfine levels to pair, with a transition temperature

$$T_c \sim T_f e^{-1/k_f |a_s|}, \quad (23)$$

with  $T_f$  is the Fermi temperature. As one moves towards the resonance,  $T_c$  grows. To the left of the resonance, pairs of atoms can fall into a weakly bound state, forming molecules; in this regime, one expects the system to consist of a Bose-Einstein condensate of these molecules. In fact, as one goes through the resonance starting from the right, the Cooper pairs in the BCS state decrease in size, and go continuously into the Bose-Einstein condensate of molecules. Bose-Einstein condensation of di-fermion molecules and BCS pairing are two ends of a continuum with no phase transition en route [57, 58, 59]. The trapped atomic systems give one the first opportunity to study this BEC-BCS crossover experimentally. The situation is remarkably similar to that discussed in color superconductivity of a quark-gluon plasma, where the color-flavor-locked state goes continuously, with decreasing baryon density, into a gas of nucleons [60]. The precise analogue would be the crossover in color-SU(2) from paired quarks at high density to Bose-condensed mesons at lower density [61].

Experiments to produce paired fermions proceed by cooling a gas of fermions in the high magnetic field state, where the interactions are weakly attractive, but the temperature is too high to have BCS pairing. By ramping the magnetic field adiabatically to below the resonance one can slide the fermions into the weakly bound state there, producing a gas of long-lived Bose-condensed molecules [62, 63, 64, 65, 66]. Such coherent molecule production is reversible, with no entropy generation. The system passes in fact through the strongly coupled BCS regime to the right of the resonance. To detect this state, Regal et al. [6] at JILA (starting with  $^{40}\text{K}$  gas at initial temperature,  $T/T_f \sim 0.08$ ) stopped the adiabatic ramp just to the right of the resonance; they then carried out a rapid ramp across the resonance, which effectively projects the fermions onto molecules. By measuring the momentum distribution of these molecules they then infer the existence of a fermion condensate in the state to the right of the resonance. Similar production of paired fermions has been carried out at Duke [7], MIT [8], and Innsbruck [9]. Theoretical predictions of the phase diagram near the BEC-BCS transition [67] agree with measurements.

### A. Direct measurements of pairing

A very important issue is how to detect pairing and superfluidity directly in ultracold Fermi gases. It should be stressed that these are distinct questions, since one can have pairing of fermions into molecules that are not condensed. Direct measurements of superfluid behavior include production of stable vortices, or other persistent current phenomena, the Josephson effect, and reduction of moments of inertia, as in superfluid helium II and nuclei with nucleon pairing. Such experiments have yet to be carried out.

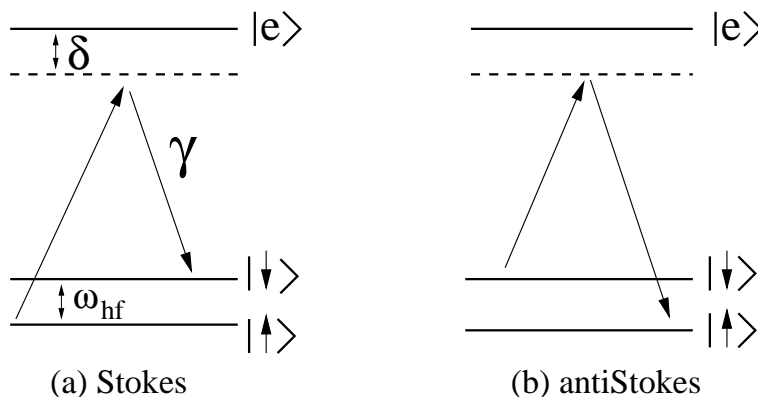


FIG. 5: (a) Stokes and (b) anti-Stokes scattering of light between two hyperfine states, as a signal of BCS pairing between the states.

Pairing can be detected by measurement, in principle, of the energy gap,  $\Delta$ , entering the quasiparticle energy,

$$E = \sqrt{(\epsilon - \mu)^2 + \Delta^2}, \quad (24)$$

where  $\epsilon$  is the energy in the absence of pairing and  $\mu$  is here the chemical potential. For example, Chin et al. [9], have trapped  $^6\text{Li}$  above a Feshbach resonance at magnetic field  $\sim 830\text{G}$ , with equal populations of atoms in the nuclear

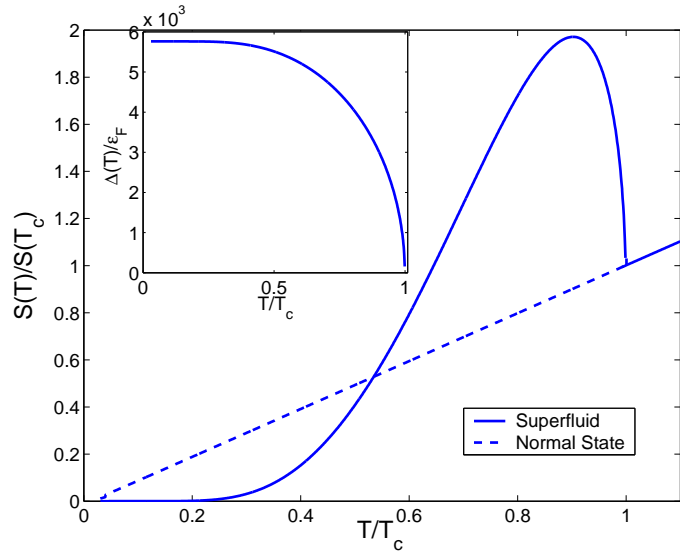


FIG. 6: Scattered light intensity as a function of temperature showing the Hebel-Slichter enhancement below  $T_c$ . The inset shows the BCS gap  $\Delta(T)$ .

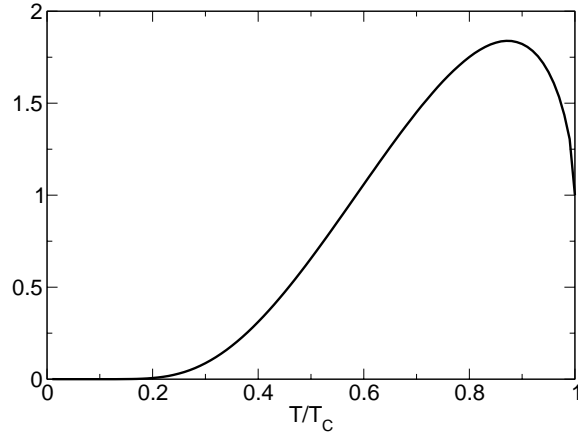


FIG. 7: Cross section for scattering of neutrinos from superfluid nuclear matter, in units of the normal state cross section, showing the Hebel-Slichter enhancement below  $T_c$ . I am very grateful to Sanjay Reddy for this figure.

spin states  $m_I = -1$  and  $0$ . At sufficiently low temperatures the atoms in the two states should be s-wave paired. By rf they excite an atom from  $m_I = 0$  to  $2$ , and find a peak in the spectrum at higher energy than would be seen for unpaired atoms; the extra energy is interpreted as that required,  $\geq 2\Delta$ , for breaking a Cooper pair. A second method of detecting pairing is through measurement of the specific heat, which shows a depression at low temperatures due to the finite gap in single particle excitation spectrum [68]. The theoretical interpretation of these measurements is given in [69]. Changes in collective mode spectra have also been interpreted as evidence for the onset of superfluidity [7, 70].

Arguably the most crucial test originally of the BCS theory of superconductivity was the Hebel-Slichter effect which demonstrated a large enhancement of the nuclear spin relaxation rate, due to coupling to paired electrons, at temperatures just below the superconducting transition temperature,  $T_c$  [71]. The peak occurs in the spin-flip spin-flip correlation function (the nuclear axial current–axial current correlation function). The analogous effect in pairing of fermions between two hyperfine levels (denoted here by  $|\uparrow\rangle$  and  $|\downarrow\rangle$ ) can be seen via laser excitation from  $|\uparrow\rangle$  to a

high-lying level,  $|e\rangle$ , off-resonance, which then de-excites to  $|\downarrow\rangle$ , with emission of a photon. The two possible processes are illustrated in Fig. 5. In the first (a) the energy of the emitted photon is less than that of the incident (Stokes scattering) and in the second (b) the emitted photon has higher energy (anti-Stokes). Figure 6 shows the expected enhancement in the rates at temperature for a weakly coupled paired system just below the superfluid transition; the enhancement is a very clear signal of the onset of pairing. Interestingly, the same effect occurs in the scattering of neutrinos from superfluid nuclear and color superconducting matter, Fig. 7, which involves the analogous nuclear axial current correlation function [73].

This research was supported in part by US National Science Foundation Grants PHY00-98353 and PHY03-55014.

- 
- [1] M.H. Anderson, J. R. Ensher, M.R. Matthews, C.E. Wieman, and E.A. Cornell, *Science* 269 (1995) 198.
- [2] K.B. Davis, M.O. Mewes, M.R. Andrews, N.J. van Druten, D.S. Durfee, D.M. Kurn, and W. Ketterle, *Phys. Rev. Lett.* 75 (1995) 3969.
- [3] C.C. Bradley, C.A. Sackett, J.J. Tollett, and R.G. Hulet, *Phys. Rev. Lett.* 75 (1995) 1687.
- [4] B. DeMarco and D.S. Jin, *Science* 340 (1999) 1087.
- [5] K.M. O'Hara, S.L. Hemmer, M.E. Gehm, S.R. Granade, and J.E. Thomas, *Science* 298 (2002) 2179.
- [6] C. A. Regal, M. Greiner, and D.S. Jin, *Phys. Rev. Lett.* 92 (2004) 040403.
- [7] J. Kinast, S. L. Hemmer, M. E. Gehm, A. Turlapov, and J. E. Thomas, *Phys. Rev. Lett.* 92 (2004) 150402.
- [8] M. W. Zwierlein, C. A. Stan, C. H. Schunck, S. M. F. Raupach, A. J. Kerman, and W. Ketterle, *Phys. Rev. Lett.* 92 (2004) 120403.
- [9] C. Chin, M. Bartenstein, A. Altmeyer, S. Riedl, S. Jochim, J. Hecker Denschlag and R. Grimm, *Science* 305 (2004) 1128.
- [10] A.B. Migdal, *Rev. Mod. Phys.* 50 (1978) 107; G. Baym, in *Nuclear Physics with Heavy Ions and Mesons, Les Houches session XXX*, R. Balian, M. Rho, and G. Ripka, eds. (North-Holland Publ. Co., Amsterdam, 1978), p. 745; G. Baym and D. K. Campbell, in *Mesons in Nuclei*, v. 3, M. Rho and D. Wilkinson, eds. (North-Holland Publ. Co., Amsterdam, 1979) p. 1031.
- [11] D. B. Kaplan and A. E. Nelson, *Phys. Lett.* B175 (1986) 57; G. E. Brown and H. A. Bethe, *Astrophys. J.* 423 (1994) 659; 506, 780 (1998); V. R. Pandharipande, C. J. Pethick, and V. Thorsson, *Phys. Rev. Lett.* 75, 4567 (1995).
- [12] J. Gasser and H. Leutwyler, *Phys. Reports*, 87 (1982) 77.
- [13] See, e.g., the talks of N. Xu, P. Braun-Munzinger, and J.-P. Blaizot on ultrarelativistic heavy ion physics in these Proceedings.
- [14] A. Krawczyk, A.G. Lyne, J.A. Gil, and B.C. Joshi, *Mon. Not. R. Astron. Soc.* 340 (2003) 1087.
- [15] G. Baym, R. Epstein, and B. Link, *Physica* B178 (1992) 1; M.A. Alpar, *Phys. Rev. Lett.* 58 (1987) 2152.
- [16] A.J. Leggett, *Rev. Mod. Phys.* 73 (2001) 307.
- [17] G. Baym and C.J. Pethick, *Phys. Rev. Lett.* 76 (1996) 6.
- [18] S. Stringari, *Phys. Rev. Lett.* 77 (1996) 2360
- [19] I. Bloch, T.W. Hänsch, and T. Esslinger, *Nature* 403 2000 166.
- [20] M. R. Andrews, C.G. Townsend, H.-J. Miesner, D.S. Durfee, D.M. Kurn, and W. Ketterle, *Science* 275 (1997) 637.
- [21] M. Greiner, O. Mandel, T. Esslinger, T. W. Hänsch, and I. Bloch, *Nature* 415 (2002) 39.
- [22] This section is based in part on G. Baym in *Proc. Quantum Fluids and Solids 2004*, *J. Low Temp. Phys.* (in press); cond-mat/0408401.
- [23] J.R. Abo-Shaer, C. Raman, J.M. Vogels, and W. Ketterle, *Science* 292 (2001) 476.
- [24] P.C. Haljan, I. Coddington, P. Engels, and E.A. Cornell, *Phys. Rev. Lett.* 87 (2001) 210403; P. Engels, I. Coddington, P.C. Haljan, and E.A. Cornell, *Phys. Rev. Lett.* 89 (2002) 100403.
- [25] I. Coddington, P. Engels, V. Schweikhard, and E. Cornell, *Phys. Rev. Lett.* 91 (2003) 100402.
- [26] V. Schweikhard, I. Coddington, P. Engels, V.P. Mogendorff, and E.A. Cornell, *Phys. Rev. Lett.* 92 (2004) 040404.
- [27] I. Coddington, P. C. Haljan, P. Engels, V. Schweikhard, S. Tung and E. A. Cornell, cond-mat/0405240.
- [28] G. Baym and C.J. Pethick, *Phys. Rev. A* 69 (2004) 043619.
- [29] U.R. Fischer and G. Baym, *Phys. Rev. Lett.* 90 (2003) 140402.
- [30] T.-L. Ho, *Phys. Rev. Lett.* 87 (2001) 060403.
- [31] G. Watanabe, G. Baym, and C. J. Pethick, *Phys. Rev. Lett.* 93 (2004) 190401.
- [32] N.K. Wilkin, J.M.F. Gunn, and R.A. Smith, *Phys. Rev. Lett.* 80 (1998) 2265; N.K. Wilkin and J.M.F. Gunn, *Phys. Rev. Lett.* 84 (2000) 6; N.R. Cooper, N.K. Wilkin, J.M.F. Gunn, *Phys. Rev. Lett.* 87 (2001) 120405.
- [33] S. Viefers, T.H. Hansson, and S.M. Reimann, *Phys. Rev. A* 62 (2000) 053604.
- [34] J.W. Reijnders, F.J.M. van Lankvelt, K. Schoutens, and N. Read, *Phys. Rev. Lett.* 89 (2002) 120401; *Phys. Rev. A* 69 (2004) 023612.
- [35] N. Regnault and Th. Jolicoeur, cond-mat/0406013.
- [36] K. Kasamatsu, M. Tsubota, and M. Ueda, *Phys. Rev. A* 66 (2002) 053606.
- [37] G.M. Kavoulakis and G. Baym, *New J. Phys.* 5 (2003) 51.1; A.D. Jackson and G.M. Kavoulakis, *Phys. Rev. A* 70 (2004) 023601; A.D. Jackson, G.M. Kavoulakis, and E. Lundh, *Phys. Rev. A* 69 (2004) 053619; G.M. Kavoulakis, G. Baym, and A.D. Jackson, *Phys. Rev. A* 70 (2004) 043603.
- [38] E. Lundh, *Phys. Rev. A* 65 (2002) 043604.

- [39] V. Bretin, S. Stock, Y. Seurin and, J. Dalibard, Phys. Rev. Lett. 92 (2004) 050403.
- [40] G. Baym, J.-P. Blaizot, M. Holzmann, F. Laloë and D. Vautherin, Phys. Rev. Lett. (1999); Euro. J. Phys. B24 (2001) 1703.
- [41] This section is based in part on G. Baym, J. Phys. B: At. Mol. Opt. Phys. 34 (2001) 4541.
- [42] P. Grüter, D.M. Ceperley, and F. Laloë, Phys. Rev. Lett. 79 (1997) 3549.
- [43] M. Holzmann and W. Krauth, Phys. Rev. Lett. 83 (1999) 2687.
- [44] P. Arnold and G. Moore, Phys. Rev. Lett. 87 (2001) 120401.
- [45] V. Kashurnikov, N. Prokof'ev, and B. Svistunov, Phys. Rev. Lett. 87 (2001) 120402.
- [46] G. Baym, J.-P. Blaizot, and J. Zinn-Justin, Europhys. Lett. 49 (2000) 150.
- [47] P. Arnold and B. Tomášik, Phys. Rev. A 64 (2001) 053609.
- [48] M. Holzmann, G. Baym, J.-P. Blaizot, and F. Laloë, Phys. Rev. Lett. 87 (2001) 120403.
- [49] P. Arnold, G. Moore, and B. Tomášik, Phys. Rev. A 65 (2002) 013606.
- [50] S.L. Cornish, N.R. Claussen, J.L. Roberts, E.A. Cornell and C.E. Wieman, Phys. Rev. Lett. 85 (2000) 1795.
- [51] J. Carlson, S.-Y. Chang, V.R. Pandharipande, and K.E. Schmidt, Phys. Rev. Lett. 91 (2003) 050401.
- [52] H. Heiselberg, J. Phys. B: At. Mol. Opt. Phys. 37 (2004) 1.
- [53] M.E. Gehm, S.L. Hemmer, S.R. Granade, K.M. OHara, and J.E. Thomas, Phys. Rev. A 68 (2003) 011401.
- [54] T. Bourdel, J. Cubizolles, L. Khaykovich, K.M.F. Magalhaes, S.J.J.M.F. Kokkelmans, G.V. Shlyapnikov, and C. Salomon, Phys. Rev. Lett. 91 (2003) 020402.
- [55] B.A. Gelman, E.V. Shuryak and I. Zahed, nucl-th/0410067.
- [56] M. Holland, S.J.J.M.F. Kokkelmans, M.L. Chiofalo, and R. Walser, Phys. Rev. Lett. 87(2001) 120406; J.N. Milstein, S.J.J.M.F. Kokkelmans, and M.J. Holland, Phys. Rev. A 66, (2002) 043604.
- [57] D.M. Eagles, Phys. Rev. 186 (1969) 456.
- [58] A.J. Leggett, J. Phys. (Paris) C7 (1980) 19.
- [59] P. Nozières and S. Schmitt-Rink, J. Low Temp Phys. 59 (1985) 195.
- [60] T. Schäfer and F. Wilczek, Phys. Rev. Lett. 82 (1999) 3956
- [61] H. Abuki, T. Hatsuda, K. Itakura, Phys. Rev. D65 (2002) 074014; K. Itakura, Nucl. Phys. A715 (2003) 859; T. Hatsuda, in these Proceedings.
- [62] K.E. Strecker, G.B. Partridge and R.G. Hulet, Phys. Rev. Lett. 91 (2003) 080406.
- [63] C. A. Regal, C. Ticknor, J. L. Bohn, and D. S. Jin, Nature 424 (2003) 47.
- [64] J. Cubizolles, T. Bourdel, S. Kokkelmans, G. Shlyapnikov, and C. Salomon, Phys. Rev. Lett. 91 (2003) 240401.
- [65] S. Jochim, M. Bartenstein, A. Altmeyer, G. Hendl, C. Chin, J. Hecker Denschlag, and R. Grimm, Phys. Rev. Lett. 91 (2003) 240402.
- [66] M.W. Zwierlein, C.A. Stan, C.H. Schunck, S.M.F. Raupach, S. Gupta, Z. Hadzibabic, and W. Ketterle, Phys. Rev. Lett. 91 (2003) 250401.
- [67] R.B. Diener and T.-L. Ho, cond-mat/0404517.
- [68] J. Kinast, A. Turlapov, and J. E. Thomas, cond-mat/0409283.
- [69] Q. Chen, J. Stajic, and K. Levin, cond-mat/0411090.
- [70] M. Bartenstein, A. Altmeyer, S. Riedl, S. Jochim, C. Chin, J. Hecker Denschlag, and R. Grimm, Phys. Rev. Lett. 92 (2004) 203201.
- [71] L.C. Hebel and C.P. Slichter, Phys. Rev. 113 (1959) 1504.
- [72] G. M. Bruun and G. Baym, Phys. Rev. Lett. 93 (2004) 150403.
- [73] J. Kundu and S. Reddy, nucl-th/0405055.